An Ultrasonically Powered Implantable Device for Targeted Drug Delivery

Jayant Charthad[1], Spyridon Baltsavias[1], Devleena Samanta[2], Ting Chia Chang[1], Marcus J. Weber[1], Niloufar Hosseini-Nassab[2], Richard N. Zare[2], and Amin Arbabian[1]

***Abstract*— A wirelessly powered implantable device is proposed for fully programmable and localized drug delivery. The implant is powered using an external ultrasonic transmitter and operates at < 5% of the FDA diagnostic ultrasound intensity limit. Drug release is achieved through electrical stimulation of drug-loaded polypyrrole nanoparticles. A design methodology for the implant electronics is presented and experimentally demonstrated to be accurate in predicting the concentration of the released drug. To the best of our knowledge, this is the first ultrasonically powered implantable device platform for targeted drug delivery using electroresponsive polymers. The active area of the implant electronics is just 3 mm × 5 mm.**

I. Introduction

Controlled and localized delivery of drugs to a specific target site in the body is one of the main challenges in drug administration today. The primary limitation of the more prevalent oral and parenteral forms of drug delivery is that drugs are systemically absorbed into the blood stream and distributed nonspecifically. This reduces their effectiveness and can potentially lead to undesired side-effects [1]. Additionally, targeted delivery into the central nervous system is necessary for treating several neurological diseases, where the blood-brain barrier limits penetration of systemically delivered drugs [2]. Wirelessly powered and controlled, minimally invasive implantable devices, loaded with the requisite drug cargo, can help to solve these problems [1].

Several implantable drug delivery devices have been proposed in the past [1], with target applications ranging from ocular disease to osteoporosis treatment. For future expansion of the application space of such devices, it is necessary to overcome several implementation issues: existing devices either include a bulky battery [3], requiring highly invasive surgery for implantation, or use RF/inductive wireless powering techniques [4], which are characterized by significant efficiency loss in millimeter (mm)-sized, deeply implanted (>5 cm) device power-up scenarios [5].

In this paper, we demonstrate the *first* ultrasonically powered implant platform for enabling fully programmable and localized drug delivery. Ultrasonic power transfer has several advantages over RF and inductive powering [5], due to which it enables miniaturization of the implant to the injectable size (mm and sub-mm dimensions), and operation at depths >5 cm inside the body. Accordingly, we envision that the overall size of our implant will depend on the quantity of drug required for a specific application, while any electronic components can be miniaturized. Further, our drug release technique is based on electrical stimulation of drug-loaded polypyrrole nanoparticles (PPy NPs) [6], [7]. This approach has two major advantages: (i) drug release from PPy is caused by partial oxidation/reduction of the polymer, allowing it to be precisely controlled by the charge (or number of electrons) injected into the polymer, and (ii) nanoparticles have an enhanced surface-to-volume ratio that allows higher drug loading compared to polymer films [7].

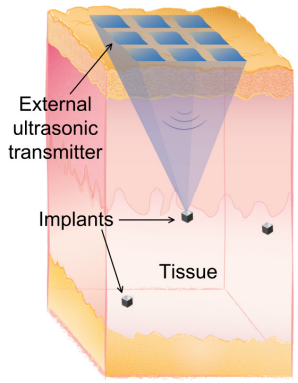

Fig 1. Conceptual representation of an ultrasonically powered implant system for controlled and localized drug delivery. The figure is not to scale.

Figure 1 shows a conceptual representation of our complete implant system. A wearable ultrasonic transmitter array can be used to locate single or multiple implants, and then beam-form energy to them. This helps with achieving a high power transfer link efficiency, and selectively controlling specific implants. In this demonstration, a single-element transmitter is used for simplicity. Our proposed implant consists of three main blocks: (i) a mm-sized piezoelectric (piezo) receiver for harvesting ultrasonic power, (ii) electronic circuits for power conditioning, data recovery, and stimulation, and (iii) a drug delivery module (DDM) consisting of electrodes interfacing with a reservoir of drug-loaded PPy NP solution. Our current proof-of-concept implant employs a simple circuit architecture using discrete electronic components to accomplish the basic desired functions, and demonstrate the feasibility of this system.

In this paper, a design methodology for maximizing the energy efficiency of the implant is also presented, and the measured results are shown to match closely with predictions. It is further demonstrated that the drug release achieved with our wirelessly powered implant is proportional to the applied

Research supported in part by NSF CAREER award ECCS-1454107, DARPA Young Faculty Award (YFA) under Grant D14AP00043, Stanford Graduate Fellowship and the Center for Molecular Analysis and Design.

[1] J. Charthad, S. Baltsavias, T. C. Chang, M. J. Weber and A. Arbabian are with the Department of Electrical Engineering, Stanford University, Stanford, California, USA. (e-mail: jayantc@stanford.edu).

[2] D. Samanta, N. Hosseini-Nassab and R. N. Zare are with the Department of Chemistry, Stanford University, Stanford, California, USA.

stimulation voltage (V_{STIM}), the stimulation interval (T_{STIM}), and the number of times the stimulus is applied (N_{STIM}). This signifies the accuracy of our first-order models, and that our technology offers multiple degrees of freedom for precisely controlling drug release, and adapting it to local physiological conditions. This could be highly desirable for a number of chronic conditions, such as treatment of malignant tumors, chronic pain, and other neurological disorders.

II. System Design

A. Drug Delivery Module (DDM)

Our drug release mechanism is conceptually explained in Fig. 2(a). First, the drug loaded PPy NPs are synthesized via a microemulsion technique [7]. Applying an electrical stimulus (e.g. a voltage) to the solution, using electrodes, results in the release of the drug from the PPy NPs.

The DDM used in this demonstration is shown in Fig. 2(b). Here, 10 µL of the drug-loaded PPy NP solution is smeared over a screen-printed electrode (SPE, DropSens) having carbon working (WE) and counter (CE) electrodes, and a Ag/AgCl reference electrode (RE). In this design, the SPE is driven as a two-electrode system, for simplicity, with the Ag/AgCl electrode acting as a shared RE/CE. The surface area of the WE is ~27 mm^2. In future versions of our implant, we envision the electrodes to be integrated on the same board as the other implant components for compactness, and the drug-loaded PPy NPs to be contained in a reservoir with a selective membrane that is only permeable to drug molecules.

A variety of drugs or compounds can be loaded and released from PPy NPs using our technique. In this study, fluorescein sodium salt (FL) is selected as a model compound for relative ease of quantification. The FL loading was calculated to be ~13 wt%. The FL-loaded NPs are stable in solution for months, and a detailed study of their properties has already been reported in [7]. As FL is a negatively charged molecule, it is expected to be released under reducing conditions. Therefore, in this demonstration, negative stimulation voltages are applied to the WE, relative to RE/CE.

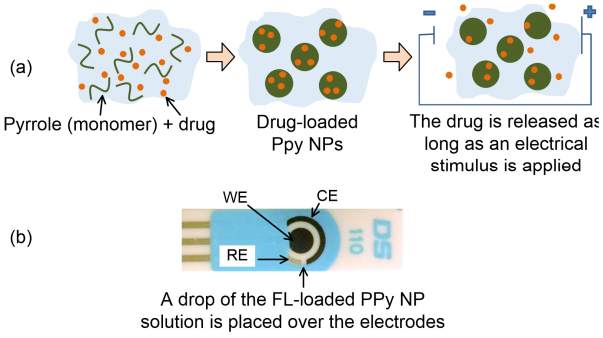

Fig 2. (a) Concept of our drug release technique, (b) the drug delivery module (DDM) used in this demonstration.

B. Equivalent Impedance Model of the DDM

In order to design the electronic circuitry of the implant, the DDM is represented by an equivalent circuit model. In general, the equivalent impedance of such an electrochemical system can be non-linear and time-variant [8]. This limits the use of traditional impedance characterization techniques in this design. Rather, more sophisticated Electrochemical Impedance Spectroscopy (EIS) measurements, along with a characterization of the time-variance of the system, would be required for obtaining a robust and scalable circuit model [8].

Here, a lookup-table-based approach is adopted for modeling the DDM by studying its input current profile for different fixed stimulation voltages, as shown in Fig. 3. To first-order, the DDM is modeled as a resistor (R_{load}), given by the ratio of the applied V_{STIM} and the *average* value of the current over 30 s. Table I shows these derived values of R_{load}, and the required average load powers ($P_{load,avg}$), for each value of V_{STIM}. It can be noted that the value of R_{load} depends on V_{STIM}, implying that the DDM is indeed non-linear. This characterization was performed using a potentiostat (Pine WaveNow). The time period for this characterization was chosen to be 30 s, because this is the typical stimulation interval required for drug release in our technique. It will be shown in section III that the wirelessly activated drug release achieved with this modeling strategy closely matches expected values.

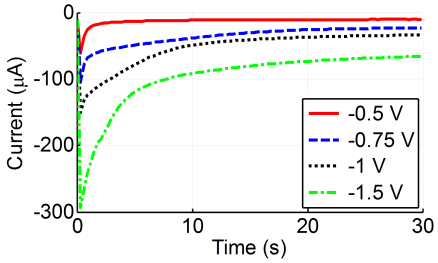

Fig 3. Measured current through the DDM for different stimulation voltages (V_{STIM}) applied to WE relative to RE/CE.

TABLE I
EQUIVALENT IMPEDANCE OF THE DDM (R_{load}) AND THE REQUIRED AVERAGE LOAD POWER ($P_{load,avg}$)

Stimulation Voltage, V_{STIM} (V)	**R_{load} (kΩ)**	**$P_{load,avg}$ (µW)**
-0.5	41.8	6.0
-0.75	22.5	25.0
-1.0	19.3	51.8
-1.5	15.4	146.1

C. Design of Implant Electronics

Figure 4 presents a circuit schematic of our implant. In addition to the piezo receiver, the implant electronics consist of a series matching capacitor (C_{match}), a commercially available bridge rectifier chip (Avago HSMS-282P) for AC-DC conversion, and a 10 nF storage capacitor (C_{stor}). Note that the DDM is interfaced such that the voltage applied to WE is negative with respect to RE/CE. In this circuit, for a given R_{load}, V_{STIM} is determined by the input power to the rectifier, which is, in turn, controlled by the input power to the external ultrasonic transmitter and the power transfer link efficiency. Further, in this design, other stimulation parameters (T_{STIM} and N_{STIM}) are determined by the duration for which the external ultrasonic transmitter is on. In future versions, a custom integrated circuit (IC) can be designed to include a voltage regulator for generating a constant output DC voltage, or a current stimulator (for precise control over injected charge), as well as more sophisticated circuits for data processing.

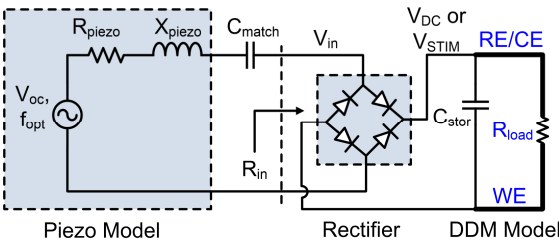

Fig 4. Circuit schematic of our implant, showing the equivalent circuit models of the piezo and the DDM.

In this demonstration, a piezoelectric transducer with a thickness of 1.44 mm and lateral dimensions of 1.02 mm × 1.02 mm is used as the receiver [5], [10]. This piezo was designed to achieve resonance near ~1 MHz to enable operation at depths > 5 cm in the body, as well as resistance (R_{piezo}) in the ~kΩ range to match to typical implant loads [5]. Unlike traditional harvesting systems, the piezo is operated *off-resonance*, between its short and open circuit resonance frequencies of 0.94 MHz and 1.28 MHz (called the "inductive band"), respectively [9]. The equivalent circuit model of the piezo in the inductive band is shown in Fig. 4. Here, V_{oc} denotes the peak open-circuit voltage of the piezo, and is a function of its electrical available power (P_{av}) and resistance (R_{piezo}) [10].

We define the total efficiency of our implant (η_{total}) as:

$$\eta_{total} = \frac{P_{load,avg}}{P_{av}} = \eta_{match} \times \eta_{rectifier} \ . \qquad (1)$$

Here, η_{match} denotes the efficiency of power transfer across the piezo-rectifier interface (related to impedance matching), and $\eta_{rectifier}$ denotes the AC-DC conversion efficiency of the rectifier. Further, the electrical available power at the piezo is given by:

$$P_{av} = I_{acou} \times A_{phys} \times PCE \ , \qquad (2)$$

where, I_{acou} is the acoustic intensity at the piezo, A_{phys} is its physical cross-sectional area normal to the incoming acoustic wave, and PCE is the power conversion efficiency of the receiver from acoustic to electrical domain [9]. Using (1) and (2), the required acoustic intensity can be written as:

$$I_{acou} = \frac{P_{load,avg}}{\eta_{match} \times \eta_{rectifier} \times PCE \times A_{phys}} \ . \qquad (3)$$

Our goal for this design is to maximize the overall efficiency of the implant, such that I_{acou} required at the piezo, for achieving successful drug release, can be minimized.

In order to maximize implant efficiency for each V_{STIM} to be applied to the DDM (Table I), it is important for the system to be reconfigurable [9]. In this design, the main control variables used for system re-configuration are: the frequency of power transfer, the input power to the external ultrasonic transmitter (which directly relates to I_{acou} at the implant for a given implant depth), and the value of C_{match} [9]. Since C_{match} cannot be easily reconfigured in our discrete-level implementation, different implant prototypes are designed, each optimized for a particular target value of V_{STIM} (i.e. having different optimal values for the control variables). The same piezo geometry and packaging (as described previously) are used for all the implant prototypes. In future IC-based versions of our implant, a single implant prototype can be optimized for different target V_{STIM} values by implementing a reconfigurable on-chip capacitor bank for tuning C_{match}.

For a given combination of V_{STIM} and R_{load} (Table I), first, simulations are performed in Agilent ADS to find the optimal value of R_{piezo} that maximizes η_{match}. Based on the measured impedance profiles of the piezos on our different prototype boards (each corresponding to a particular target V_{STIM}), the optimal operating frequency (f_{opt}) in the inductive band is found for achieving this value of R_{piezo}. Next, C_{match} is chosen to cancel the inductive reactance of the piezo (X_{piezo}) at f_{opt} [9]. From these simulations, we can also estimate the minimum required P_{av} for supporting a given load. Based on the measured PCE (~0.6) of our piezos at f_{opt}, (3) is then used to estimate the minimum required I_{acou} for powering a given load. In section III, these estimated values of I_{acou} will be compared with those required during measurements, for validating our design strategy.

Table II shows the optimal parameters for each value of V_{STIM}, obtained from the above design strategy. Note that even though the optimal R_{piezo} is monotonic with the target V_{STIM}, f_{opt} and C_{match} are not, owing to slight board-to-board variations in the impedance profile of the piezos.

TABLE II

DESIGN PARAMETERS FOR MAXIMIZING THE EFFICIENCY OF THE IMPLANT SYSTEM FOR EACH STIMULATION VOLTAGE (V_{STIM}) APPLIED TO THE DDM

V_{STIM} (V)	R_{load} (kΩ)	R_{piezo} (kΩ)	f_{opt} (MHz)	C_{match} (pF)	P_{av} (μW)	Estimated I_{acou} (mW/mm²)
-0.5	41.8	48.6	1.21	2.1	10.5	0.02
-0.75	22.5	25.2	1.18	3.7	38.9	0.06
-1.0	19.3	21.4	1.19	3.3	78.2	0.12
-1.5	15.4	15.6	1.17	4.2	189.5	0.29

III. MEASUREMENT RESULTS

In order to demonstrate the capability of our proposed implant, *in vitro* experiments are performed using the measurement setup shown in Fig. 5. All components of the implant electronics are integrated on an FR4 printed circuit board (PCB) with a total active area of just 3 mm × 5 mm. In this demonstration, the output of the rectifier is routed outside the tank, and connected to the DDM. Wireless power transfer is achieved at a separation of 6 cm between the external ultrasonic transmitter (Olympus A303S-SU) and the implant.

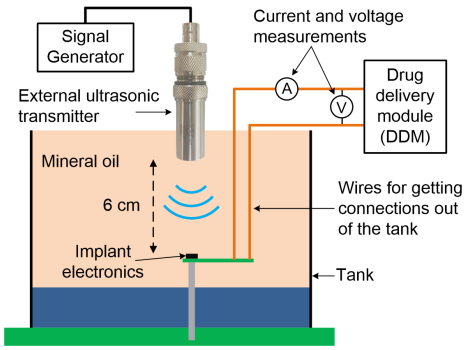

Fig 5. Experimental measurement setup.

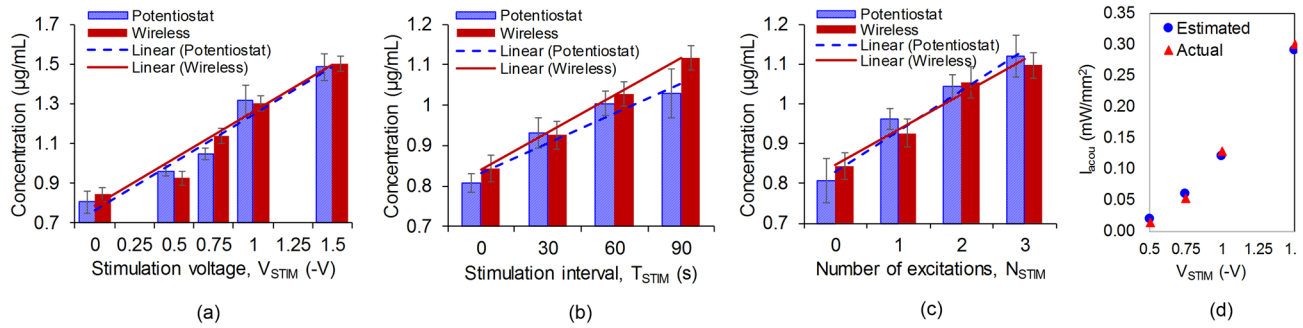

Fig. 6. Measured concentration of released drug achieved with our wireless implant, benchmarked against that achieved with a potentiostat, for different values of: (a) V_{STIM} (T_{STIM} = 30 s, N_{STIM} = 1), (b) T_{STIM} (V_{STIM} = -0.5 V, N_{STIM} = 1), and (c) N_{STIM} (V_{STIM} = -0.5 V, T_{STIM} = 30 s, T_{GAP} = 30s); (d) Comparison between actual acoustic intensities used during our measurements and the estimated values in Table II.

Mineral oil is used as a coupling medium in order to minimize the electrical parasitics, and because its acoustic impedance is similar to that of soft tissues. In a real scenario with non-homogeneous tissue and propagation losses, beamforming can be used to focus ultrasonic energy at the implant [11]. After stimulating the DDM with the desired parameters, drug release is quantified by diluting the PPy NP solution with water to 200 µL, centrifuge filtering the sample, and monitoring the absorbance of the filtrate.

Fig. 6(a)-(c) show measurement results for ultrasonically controlled drug release using our implantable device, benchmarked against measurements where the DDM is directly driven with a benchtop potentiostat. For characterizing the effect of V_{STIM}, the stimulus was applied for a fixed T_{STIM} of 30 s (Fig. 6(a)). The effect of T_{STIM} was characterized by applying a fixed V_{STIM} (-0.5 V) for different durations ranging from 0 s to 90 s (Fig. 6(b)). Similarly, the effect of the N_{STIM} was characterized by applying 0-3 excitations of a fixed V_{STIM} (-0.5 V) and a fixed T_{STIM} (30 s), with a gap (T_{GAP}) of 30 s between two consecutive excitations (Fig. 6(c)).

It can be noted that the concentration of the released drug is approximately linearly related to V_{STIM}, T_{STIM} and N_{STIM}. This signifies that these parameters can be used for defining multi-dimensional stimulation patterns for precisely controlled drug release, depending on the required dosage for a particular application. Further, these results demonstrate that the drug release profiles achieved with the wireless implant system closely match those achieved with the potentiostat, signifying that our modeling and design strategies are sufficiently accurate. The slight difference in the linear profiles of Fig. 6(b) is due to the unregulated voltage in our wireless experiments. Uncertainty for each data point corresponds to one standard deviation over three measurements. The FL leakage observed in the absence of electrical stimulation occurs as the PPy NPs are pH-sensitive [7]. However, this free leakage is <5% of the total incorporated drug.

Finally, in Fig. 6(d), it is shown that the acoustic intensities required during measurements closely match estimated values from Table II. These intensities are based on the characterization of our transmitter using a wideband needle hydrophone (Onda HNC-1500). It can be noted that I_{acou} is within 5% of the FDA diagnostic ultrasound intensity limit of 7.2 mW/mm^2, emphasizing that our device has sufficient safety margin [12]. Future work for our device involves complete integration, bio-compatible packaging, and *in vivo* experiments to demonstrate its efficacy in animal models. Further, a bio-sensor can also be integrated to implement a closed-loop, adaptive drug delivery system.

IV. Conclusion

This work demonstrates the first proof-of-concept of an ultrasonically powered implantable device for targeted drug delivery using nanoparticles of electroresponsive polymers (polypyrrole). Ultrasonic powering enables our implant electronics to be miniaturized to an active area of just 3 mm × 5 mm, and operation at depths > 5 cm, while being well within the safety limits. Through measurements of the wirelessly powered implant, a linear relationship has been demonstrated between the concentration of the released model drug (FL) and different electrical stimulation parameters (V_{STIM}, T_{STIM} and N_{STIM}). A design strategy for maximizing the energy efficiency of the implant was also presented, and demonstrated to be sufficiently accurate in predicting drug release.

Acknowledgment

The authors thank the Stanford System-X Alliance, Rohde&Schwarz, and Agilent for the use of ADS.

References

[1] L. W. Kleiner, *et al.*, "Evolution of implantable and insertable drug delivery systems," *J. Control. Release*, vol. 181, no. 1, pp. 1–10, 2014.

[2] J. M. Blakeley, "Drug delivery to brain tumors," *Curr Neurol Neurosci Rep.*, vol. 29, no. 6, pp. 997–1003, 2012.

[3] R. Farra, *et al.*, "First-in-human testing of a wirelessly controlled drug delivery microchip," *Sci. Transl. Med.*, vol. 4, no. 122, pp. 1-10, 2012.

[4] R. Sheybani, *et al.*, "Wireless programmable electrochemical drug delivery micropump with fully integrated electrochemical dosing sensors," *Biomed. Microdevices*, vol. 17, no. 4, p. 74, 2015.

[5] J. Charthad, *et al.*, "A mm-sized implantable medical device (IMD) with ultrasonic power transfer and a hybrid bi-directional data link," *IEEE J. Solid-State Circuits*, vol. 50, no. 8, Aug. 2015.

[6] J. Ge, *et al.*, "Drug release from electric-field-responsive nanoparticles," *ACS Nano*, vol. 6, no. 1, pp. 227–233, 2012.

[7] D. Samanta, *et al.*, "Electroresponsive nanoparticles for drug delivery on demand," *Nanoscale*, vol. 8, no. 21, pp. 9310–317, 2016.

[8] A. J. Bard and L. R. Faulkner, *Electrochemical Methods: Fundamentals and applications*, 2001.

[9] T. C. Chang, *et al.*, "Design of high-efficiency miniaturized ultrasonic receivers for powering medical implants with reconfigurable power levels," in *IEEE Int. Ultrasonics Symposium (IUS)*, Oct. 2015.

[10] M. J. Weber, *et al.*, "A miniaturized ultrasonically powered programmable optogenetic stimulator system," in *Proc. IEEE Biomed. Wireless Technol., Networks, Sensing Syst. Top. Conf.*, Jan. 2016.

[11] F. Mazzilli, *et al.*, "A 10.5 cm ultrasound link for deep implanted medical devices," *TBIOCAS*, 2014, 8, (5), pp. 738–750.

[12] "Information for Manufacturers Seeking Marketing Clearance of Diagnostic Ultrasound Systems and Transducers," Food and Drug Administration, Rockville, MD, 2008.